Infectious Disease Modelling 10 (2025) 477–492

Contents lists available at ScienceDirect

Infectious Disease Modelling

journal homepage: www.keaipublishing.com/idm

A modelling approach to characterise the interaction between behavioral response and epidemics: A study based on COVID-19

Xinyu Chen , Suxia Zhang *, Jinhu Xu

School of Science, Xi'an University of Technology, Xi'an, 710048, PR China

A R T I C L E I N F O

Article history:
Received 25 September 2024
Received in revised form 24 November 2024
Accepted 17 December 2024
Available online 26 December 2024
Handling Editor: Dr. Raluca Eftimie

Keywords:
Mathematical model
Human behavioral response
Disease transmission
Particle swarm optimization
COVID-19

A B S T R A C T

During epidemic outbreaks, human behavior is highly influential on the disease transmission and hence affects the course, duration and outcome of the epidemics. In order to examine the feedback effect between the dynamics of the behavioral response and disease outbreak, a simple SIR-β type model is established by introducing the independent variable β of effective contact rate, characterizing how human behavior interacts with disease transmission dynamics and allowing for the feedback changing over time along the progress of epidemic and population's perception of risk. By a particle swarm optimization algorithm in the solution procedures and time series of COVID-19 data with different shapes of infection peaks, we show that the proposed model, together with such behavioral change mechanism, is capable of capturing the trend of the selected data and can give rise to oscillatory prevalence of different magnitude over time, revealing how different levels of behavioral response affect the waves of infection as well as the evolution of the disease.

1. Introduction

Epidemics and pandemics have always been a major threat to humanity throughout history and have seriously endangered public health, social and economic development, such as the COVID-19 pandemic that emerged in late 2019 and spread rapidly around the world, causing more than 6.9 million deaths and disruption to normal functioning of society. The outbreaks and recurrences of infectious diseases have reminded the world of the importance of uncovering the underlying mechanisms that influence disease transmission and have sparked a sustained interest in the dynamic modelling (Azizi, Kazanci, Komarova, & Wodarz, 2022; Hethcote, 2000; Panicker & Sasidevan, 2024). Mathematical modelling of viral epidemics, basically including deterministic modelling and stochastic modelling, allows for an understanding of the transmission dynamics in order to assist in controlling and preventing the spread of diseases (Laarabi, Rachik, Kahlaoui, & Labriji, 2013; Wang & Zhang, 2024; Yerlanov, Agarwal, Colijn, & Stockdale, 2023).

In epidemiological literature, a wide range of mathematical models have been developed to explain, characterise and project the evolution of different infectious diseases, such as compartmental models (Gilbert et al., 2020; Wang, Wu, & Tang,

* Corresponding author.
E-mail address: zsuxia@163.com (S. Zhang).

https://doi.org/10.1016/j.idm.2024.12.013

2022), agents-based models (Panicker & Sasidevan, 2024), network-based models (Stolerman, Coombs, & Boatto, 2015) and machine learning-based models (Song & Xiao, 2022a; Yin, Wu, & Song, 2023). Compartment model, starting from the pioneering epidemiological model introduced by Kermack & McKendrick, 1927 (Kermack & McKendrick, 1927), is a well established approach to describing and simulating the evolution of an epidemic within a population. In general, such models are based on the concept that the population can be divided into disjoint groups (e.g. susceptible, infected and removed) according to their ability to host and transmit a pathogen, and the spread of the disease is then modeled by a system of differential equations that describe how people move from different compartments.

When using a compartment model to describe the transmission of a specific virus, it requires the knowledge of the parameters defining the flows from one compartment to another, some of which can be estimated directly from the available data while others cannot be easily estimated. For instance, the infection rate (also called as force of infection), which can be decomposed in terms of the average rate of contact between individuals per unit time (the contact rate) and the average probability of infection per contact (the intrinsic infection rate), depends on both biological and societal conditions and thus is time-varying. During an epidemic outbreak, public health authorities may be forced to impose and promote restrictive measures, such as social distancing, quarantine, and other non-pharmaceutical interventions (NPIs), with the aim of changing the behavior of the population and, consequently, the course of the epidemic (Bedson et al., 2021; Haug et al., 2020). These restrictive measures may be tuned alternatively tight or relax over time, depending on fluctuations in the contagion data, and on economic and social costs of their implementation. In addition, the epidemic state may also lead individuals to spontaneously change their social behavior, i.e., to reduce or increase interactions according to their perception of the risk of being infected (Cabrera, Córdova-lepe, Gutiéerrez-Jara, & Vogt-Geisse, 2021; Rubin, Amlôt, Page, & Wessely, 2009). It is well accepted that such changes in human behavior, including self-regulated and policy-driven, play an important role in reducing disease transmission and mitigating the impact of the epidemics at a population level, even in the absence of pharmaceutical interventions. As a result, modelling human behavior within mathematical epidemiological models and accounting for the consequences of behavior modification on the dynamics has been a recent focus of model-based analysis (Brankston et al., 2024; Diagne et al., 2024; Fome et al., 2023; Zhang, Scarabel, Murty, & Wu, 2023; Zhou, Rahman, Khanam, & Taylor, 2023; Zuo, Ling, Zhu, Ma, & Xiang, 2023).

In a pandemic situation, when the transmission is driven by human contact behavior, both the implementation of NPIs that are highly dependent on human behavior and voluntary avoidance behavior by individuals, serve as critical tools to alter the course, duration and outcome of disease outbreaks, regardless of the availability of vaccines. On the other hand, the emerging viral infectious disease will necessarily motivate authorities to impose NPIs and the population to modify their behavior in direct response to the risk of high prevalence or persistent deterioration. For example, the increased number of infections will result in a reduction in social activity and hence a decrease in the transmission rate. It is thus clear that there exists a feedback loop between the dynamics of the epidemic and the behavioral response, both at the institutional and personal level, and that this feedback may change over time along the progress of epidemic and people perception of risk and the severity of disease outbreak. Study of this feedback mechanism is a precursor to guiding public health interventions and has attracted great interest among researchers (Tang, Zhou, Wang, Wu, & Xiao, 2022; Vrugt, Bickmann, & Wittkowski, 2021). Mathematically, incorporating such interactions between epidemic outbreaks and human behavior into model variables or parameters is challenging because the adoption of protective behavior involves abstract and complex psychological and subjective factors, such as emotion of fear and awareness of disease risk (Jain, Bhaunagar, Prasad, & Kaur, 2023; Sardar, Nadim, & Rana, 2023), and the type and degree of behavior modification varies with age structure, gender and other socio-demographic characteristics (Wang et al., 2022; Zuo et al., 2023). Nonetheless, it is well established that mathematical modelling can be of great help in exploring the behavioral change mechanisms and in characterizing how human behavior interacts with disease transmission dynamics.

Mathematical models that study the spread of infectious diseases related to human behavior have received much attention. According to the principles used in modelling, there are three main approaches to the representation of feedback effects in models of transmission dynamics. One common approach is to change parameters in compartmental models from constant to non-constant, typically the transmission term, in this way modelling the feedback from disease transmission to human behavioral response. In such context, different forms of nonlinear function have been used to describe the time varying nature of the effective contact rate β. For example, a saturated function $\beta(t) = \frac{\beta_0}{1+kI(t)}$ was given by Capasso and Serio (Capasso & Serio, 1978), where I is the number of infectious individuals and β_0 is the nominal contact rate, to account for the psychological effect in the population, that is, more self-protective behavior at high levels of I. Exponential decay function $\beta(t) = \beta_0 e^{-\alpha_1 E - \alpha_2 I - \alpha_3 H}$ and $\beta(t) = \beta_0(1 - e^{-aI})$ were presented in (Kolokolnikov & Iron, 2021; Liu, Wu, & Zhu, 2007) to reflect the impact of for instance, social media and mask wearing on the regulation of transmission likelihood, where E and H denoted the exposed and hospital population, respectively. Additionally, Xiao et al. (Xiao, Tang, & Wu, 2015) introduced a piece-smooth function that depends on both I and its derivative, which induces an impact switch of media coverage on the contact rate. There are other articles incorporating similar nonlinear function in transmission term, see (Cui, Sun, & Zhu, 2008; Song & Xiao, 2022b; Sun, Yang, Arino, & Khan, 2011; Tchuenche & Bauch, 2012; Tchuenche et al., 2011) and references therein. A second approach to modelling feedback is to divide the population into more different sub-populations, such as risk-aware and risk-unaware compartments, based on individuals' awareness, risk perception or activity level, see (Agaba, Kyrychko, & Blyuss, 2017; Funk, Gilad, & Jansen, 2010; Teslya et al., 2020) for example. Specifically, an SIRS-type model that included private awareness arising from direct contacts between populations and public awareness stemming from information campaigns can be seen in (Agaba et al., 2017), which studied how these two types of awareness affect the dynamics of

the disease spread. On the other hand, the authors in (Teslya et al., 2020) developed a compartmental model that stratified the population by disease status and disease awareness status to compare the individual and combined effectiveness of self-imposed measures and government-imposed social distancing in mitigating, delaying, or preventing the COVID-19 epidemic. Another approach to incorporating the feedback is to describe the pandemic as an interaction between two types of dynamical processes, the compartmental component corresponding to disease dynamics and the regulatory component corresponding to behavioral response dynamics (Buonomo, Della Marca, & Sharbayta, 2022; Song & Xiao, 2019). More specifically, such category of models has been proposed with extra compartment, such as the amount of media coverage (Wang & Zhang, 2024) and an information index related to disease prevalence (Bulai, Montefusco, & Pedersen, 2023), and this way allows to understand the epidemiological role of behavior modification as a regulatory variable.

In this paper, we propose a deterministic SIR-β model that extends the classical Susceptible-Infectious-Removed (SIR) model by introducing the rate of contact change due to individuals' behavioral response, which makes it possible to capture the feedback effects in two directions, namely the impact of behavioral change on disease dynamics and that of disease transmission on behavior dynamics. In addition, the structure of this model remains simple enough for analytical and computational tractability, while preserving important modelling properties and considering the balance between complex social and behavioral phenomena and their corresponding mathematical quantification. In order to improve the performance of the predictions conerning the number of infected individuals and their evolution over time, which depends to a large extent on the precise knowledge of the model parameters, we adopt a particle swarm optimization (PSO) algorithm to invert the model parameters, which allows us to use COVID-19 data to approximate the underlying SIR-β epidemic parameters. To verify the validity of our proposed model, we fit the COVID-19 data to the disease course over different durations in four countries, where the shape of the infection curves showed different characteristics of change after the initial outbreak, with some experiencing multiple individual peaks. The fitting results reveal that the model is capable of capturing the trend of the data, and the potential impact of variation in behavior-related parameters on mitigating the disease spread is explored.

The contents of the paper are as follows. In Section 2, we propose the materials and methods. In Section 3, the results are presented. Section 4 gives the summary and discussion.

2. Materials and methods

2.1. Data collection

From the publicly available source (World Health Organization), we acquire four time series of COVID-19 data (hereafter referred to as Data 1, Data 2, Data 3 and Data 4), characterised by different shapes of the infection curves, to examine the pandemic waves in both short and relatively long time periods. In particularly.

- Data 1 is obtained from the pandemic wave in Shanghai, China from January 22, 2020 to February 12, 2020, during which a singe wave of infection occurs.
- Data 2 in Armenia runs from April 11, 2020 to January 6, 2021 and features two waves of infection, with the first peak followed by a much higher one.
- In contrast, Data 3 in Lithuanian from September 8, 2020 to June 3, 2021 exhibits two waves of infection, but the second peak is much lower than the first one.
- On the other hand, Data 4 in Jamaican runs from December 21, 2020 to December 21, 2021 and experiences two waves of infection of similar magnitude.

2.2. Model formulation

To incorporate human behavioral change mechanism, we extend the classical SIR model as the SIR-β type model, which includes the compartment of dynamic variable β, to describe the evolution of human behaviors. As in the SIR model, assuming that in the region under consideration, $N(t)$ denotes the total population at time t, which is divided into three disjoint sub-populations, i.e., the susceptible $S(t)$, the infected $I(t)$ and the removed $R(t)$, respectively. The variable $\beta(t)$ refers to the time-varying infection rate, by which the susceptible individuals in healthy state contract the disease from any infected individual, depending on both biological and societal conditions, as highlighted previously, and it therefore functionally links changes in behaviors to the spread of disease transmission. The sizes of $S(t)$, $I(t)$, $R(t)$ and $\beta(t)$ at time t constitute four state variables of the proposed model. When regulating the dynamics of the behavioral response, the evolution of $\beta(t)$ has the following assumptions and characteristics.

In the absence of the disease, let β_0 be the baseline value of the infection rate. Following the emergence of an epidemic, the self-regulated and policy-driven behavior modifications to avoid being infected result in a nonlinear transmission rate, which causes the infection rate β to vary in a direction opposite to that of infections I. However, the implications of people's intrinsic resistance to change habitual behaviors and the natural tendency to return to normal life cannot be neglected when describing the dynamics of the behavioral change mechanism. Consequently, a general function $f(I, \beta, \beta_0)$ can be used initially to express the variation of β first, i.e.,

$$\beta'(t) = f(I, \beta, \beta_0),$$

where the importance of the behavioral response is modulated by the level of infection, or alternatively by other values of disease prevalence such as hospitalizations and deaths. If $I = 0$, then β tends to approach β_0, meaning that the social contact between individuals returns to its normal state in the absence of epidemic perturbations. For example, it can be quantified by the following simple form of linear equation

$$\beta'(t) = \alpha(\beta_0 - \beta),$$

here the parameter α measures the rate at which people resist changing their social behavior, and also denotes the time scale of behavior change. In this scenario, there is no disease to respond to, and thus the population will tend to follow its natural behavior patterns as long as $\beta \neq \beta_0$. On the contrary, the emergence of an epidemic will drive people to reduce their social contacts and maintain the altered behaviors, then a new reduced level of desired contact will occur, modulated by I, say with a popular form of $\frac{\beta_0}{1+(\frac{I}{I_c})^k}$, where $k \geq 1$ determines the sharpness of the behavior changes in the force of infection. $k = 1$ is the Michaelis-Menten expression, and as k increases, individuals will become more sensitive to disease prevalence. I_c is the half-saturation constant for the impact of infected cases on behavior modification, reflecting to some extent individuals' perception of the severity of the disease. For simplicity, if the Michaelis-Menten form is specifically chosen to characterise the effect of behavioral feedback on the transmission rate, given its ability to describe how society responds to the spread of COVID-19, then the dynamics of behavioral feedback becomes

$$\beta'(t) = \alpha(\frac{\beta_0}{1 + \frac{I}{I_c}} - \beta).$$

An SIR model is a simple but powerful model where the transition of individuals flows from susceptible class S to infectious class I and then to removed class R. On a relatively short time scale, demographic effects (both new births and deaths) are generally neglected in some models, and travel restrictions are also assumed to be completely enforced during an epidemic. In fact, some of the data we collected cover a longer time scale, and the engagement of individuals in avoiding public transport during the periods varied according to the prevalence, therefore the proposed model includes demographic processes to allow for any possible account of the feedback between the disease dynamics and the behavioral response dynamics. The interactions of the disease transmission and the behavioral change are illustrated in Fig. 1. Base on these assumptions, we extend the classical SIR model to include a behavioral feedback compartment, i.e., a SIR-β type model, as follows:

$$\begin{cases} \dfrac{dS}{dt} = \Lambda - \beta SI - (\mu + \delta)S, \\ \dfrac{dI}{dt} = \beta SI - (\mu + \theta + \gamma)I, \\ \dfrac{dR}{dt} = \gamma I + \delta S - \mu R, \\ \dfrac{d\beta}{dt} = \alpha\left(\dfrac{\beta_0}{1 + \dfrac{I}{I_c}} - \beta\right), \end{cases} \tag{1}$$

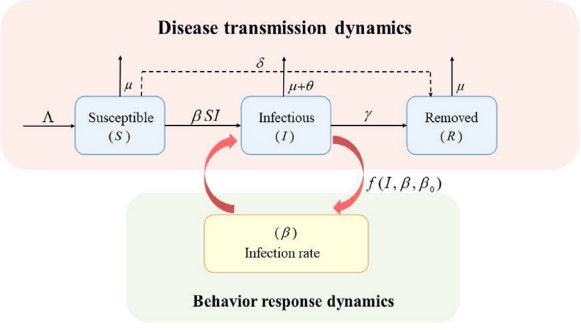

Fig. 1. Flowchart of state variables and interactions between the two dynamics.

where Λ represents the recruitment rate of the susceptible population and μ stands for the natural death rate per capita, assuming that each compartment of disease transmission dynamics has the same natural death rate. θ is the corresponding mortality rate of the disease. At the end of 2020, vaccines for COVID-19 has been approved. To capture the combined control efforts in the presence of pharmaceutical and non-pharmaceutical interventions in the prolonged outbreaks, vaccination has been considered and δ denotes the effective immunization rate of the susceptible population following vaccination. The parameter γ denotes the proportion of infected individuals recovering in unit time. From a practical point context, each parameter in model (1) is assumed to be non-negative.

For convenience, let $\alpha\beta_0 = \beta_1$, $1/I_c = c$. Since R does not appear in the equations of other variables, implying that the equation for $\frac{dR}{dt}$ has no effect on the dynamics of the model system, we will focus on the following reduced model in the remaining analysis:

$$\begin{cases} \dfrac{dS}{dt} = \Lambda - \beta SI - (\mu + \delta)S, \\ \dfrac{dI}{dt} = \beta SI - (\mu + \theta + \gamma)I, \\ \dfrac{d\beta}{dt} = \dfrac{\beta_1}{1 + cI} - \alpha\beta. \end{cases} \tag{2}$$

Remark 1. The maximum positive invariant set of model (2) gives

$$\Omega = \left\{ (S, I, \beta) \in \mathbb{R}^3_+ : 0 \le S, I \le \frac{\Lambda}{\mu},\ 0 < \beta \le \frac{\beta_1}{\alpha} \right\}.$$

The basic reproduction number is an important index which is used to measure the speed and scale of disease transmission. Using the next generation matrix approach, the basic reproduction number of system (2) can be defined as

$$\mathcal{R}_0 = \frac{\beta_1 \Lambda}{\alpha(\mu + \delta)(\mu + \theta + \gamma)}.$$

Remark2. The determination of asymptotic behaviors of the solutions for system (2) is supplemented in Appendix, which is one of the main concerns in the dynamic analysis of epidemiological models and is typically based on the stability of the associated equilibria.

2.3. Description PSO for SIR-β model

In the solution procedures, the PSO algorithm is employed to determine the parameters of the SIR-β model adopted to fit the four time series of COVID-19 data. The PSO is a population-based stochastic approach proposed by Eberhart and Kennedy in 1995, which has its roots in the simulation of the collective behaviors of birds in flocks and belongs to the class of swarm intelligence techniques. Particles in PSO move in the search space of an optimization problem and search for better positions by changing their velocity according to the rules that govern the movement of the particles. In fact, the position of a particle represents a candidate solution to the optimization problem at hand, and the rules can be seen as a model of social behavior in which particles adjust their beliefs and attitudes to match those of their peers. Due to its strong adaptability characteristics such as concise and easy to implement good robustness, the PSO algorithm has been successfully applied to a wide range of optimization problems. In our work, the PSO algorithm is employed in the estimation procedure, which consists of obtaining the parameters of the SIR-β model (β_1,c,α,Λ,μ,θ,γ,δ) by iteratively minimizing the difference between a population of possible solutions and the released data.

In our optimization, the search space is accordingly assumed to be eight-dimensional, and the position and velocity of particle i are denoted as vector $X_i = (X_{i1}, X_{i2}, \ldots, X_{i8})$ and vector $V_i = (V_{i1}, V_{i2}, \ldots, V_{i8})$, respectively. The best position that the ith particle (pbest) has ever visited is represented by $P_i = (P_{i1}, P_{i2}, \ldots, P_{i8})$, and that of the whole swarm (gbest) is $G_i = (G_1, G_2, \ldots, G_8)$. In the simulation, we define the fitness function as the following

$$f(\beta_1, c, \alpha, \Lambda, \mu, \theta, \gamma, \delta) = \sum \frac{(J_{pre} - J_{act})^2}{J_{act}}, \tag{3}$$

here J_{pre} is the simulated value of the proposed SIR-β model and J_{act} is the reported data. (3) is a reference to the chi-square statistic in the goodness-of-fit test. The update rules and the pseudocode are presented in Table 1.

Table 1
Pseudocode of PSO in simulation of model (2).

Algorithm	PSO
Input	Maximum number of iterations N_{max}, number of particles $particlesize$ number of independent variables in fitness function $narvs$, learning factors c_1, c_2, inertial parameter ω, particle velocity v, maximum particle velocity v_{max}, particle position x, threshold E
Output	Best solution $x(i,j)$, $j = 1, 2, \cdots, 8$
	$v = rand(particlesize, narvs)$, $x = rand(particlesize, narvs)$ // Initialization
	$pbest\_x = x$, $pbest\_faval = f$ //Calculating the fitness
	$[gbest\_faval, i] = \min(pbest\_faval)$
	$gbest\_x = pbest\_x(i,:)$
	while $(k \leq N_{max})$ **do** //Main loop
	for i=1:$particlesize$ **do** // Velocity update
	$v(i,:) = \omega * v(i,:) + c1 * rand * (pbest\_x(i,:) - x(i,:))$
	$+c2 * rand * (gbest\_x - x(i,:))$
	for j=1:$narvs$ **do** // Determining if flying faster than the maximum speed
	if $v(i,j) > v_{max}$ **then** $v(i,j) = v_{max}$ **end if**
	if $v(i,j) < -v_{max}$ **then** $v(i,j) = -v_{max}$ **end if**
	$m = x(i,:)$, $x(i,:) = m + v(i,:)$ // Position update
	if $x(i,1) > 4$ **then** $x(i,1) = 4$ **end if** // Limiting search space, an example
	if $x(i,1) < 3.5$ **then** $x(i,1) = 3.5$ **end if**
	if $gbest\_faval < E$, **then** // Solution update
	end if
	$k = k + 1$
	end while
	$xbest = gbest\_x$

2.4. Runge-Kutta technique for model (2)

The classical Runge-Kutta method is a common technique for numerical solution of ordinary differential equations, using a trial step at the midpoint of an interval to cancel out lower-order error terms. In view of the simplicity and robustness, the fourth-order formula (known as RK4) is adopted to simulate the dynamical behavior of model (2). For an initial value problem $y' = f(t, y(t))$ with $f : \Omega' \subset \mathbb{R} \times \mathbb{R}^n \to \mathbb{R}^n$ and $y(t_0) = y_0$, the RK4 formula is

$$
\begin{aligned}
k_1 &= hf(t_n, y_n),\\
k_2 &= hf\left(t_n + \frac{1}{2}h, y_n + \frac{1}{2}k_1\right),\\
k_3 &= hf\left(t_n + \frac{1}{2}h, y_n + \frac{1}{2}k_2\right),\\
k_4 &= hf(t_n + h, y_n + k_3),\\
y_{n+1} &= y_n + \frac{1}{6}(k_1 + 2k_2 + 2k_3 + k_4).
\end{aligned}
$$

3. Results

This section presents the parameters retrieved by solving the proposed optimization problem and the effectiveness of the SIR-β model, using the time series of COVID-19 pandemic waves from Data 1 to Data 4. The estimated parameters are listed in

Table 2
Optimized parameters for the SIR-β model by the data sample.

Data	Parameter							
	β_1	c	α	Λ	μ	θ	γ	δ
1	0.86	0.44	0.05	211200	0.0467	0.758	0.09	0
2	3.51	2.1	0.0023	17700	0.0235	0.3	0.02	0
3	8.8	0.29	0.0044	45800	0.14	0.21	0.15	0.0016
4	2.4	2.7	0.0024	10730	0.0198	0.3	0.004	0.006

Table 2, noting that the effective population size is basically difficult to measure (Yerlanov et al., 2023), and that the natural death rate and the mortality rate are also difficult to distinguish during the outbreak of COVID-19 pandemic. Moreover, the simulation results, including the best solution, the profile for the variable β and the model trajectories with different parameter scales, are given in Figs. 2–6.

3.1. Model fitting to COVID-19 cases

The parameters of the SIR-β model that best fit the time series of infected individuals in Data 1, calculated from 50 iterations of the PSO algorithm, are listed in Table 2. Note that there is no vaccine available during this period, hence there is no transition from the susceptible class to the removed class due to effective immunization. Meanwhile, for the fitness function (3), the parameter pairs that achieve its minimization are marked by red dots, as shown in Fig. 2. Consequently, the model fitting curve for Data 1 can be plotted to demonstrate how the trajectory for the daily cases matches the observed values. In fact, Fig. 2 shows that the deviation of the model trajectory from actual data is small, which is indicative of a good fit.

The reported COVID-19 Data 2 versus the fits and predictions by our proposed model is plotted in Fig. 3. The fitting curve reveals the effectiveness of our proposed model (2), from which we can see that the evolved trend of the reported data can be captured, although the deviation from the actual data exists. In particular, there is a lag between the fitting and the collected data at the first peak, and the predicted population falls below the measured fraction of the daily new cases at the second peak. For Data 3, where the second wave peak is much lower than the first one, the profile for the simulated cases is depicted in Fig. 4. Indeed, it can be visualized from the model simulation that the fitting is not accurate enough. For example, there is an obvious deviation of the predicted results from the first wave peak and the propagation at the end of the time interval. However, it does show that the fit for this type of infection event in Data 3 is improved from that in Data 2 when compared to Fig. 3. The simulation results and Data 4 are plotted in Fig. 5. The illustrations show that in terms of this type of collected data, which is characteristic of two waves of infection with similar magnitude, the fitting curve falls below the two infection peaks, especially at the second one. In fact, it should be acknowledged that the data in this prolonged period experiences a relatively complicated fluctuation, which necessarily leads to a complicated evolution of the two dynamical processes and, in turn, increases the difficulty of the fitting.

The simulation results in Fig. 2–5 demonstrate that our proposed approach is suitable for representing the feedback effect between the disease transmission and the behavioral response. Despite the complexity of the interaction between these two dynamical processes, the established modelling can be of help in exploring and characterizing the coupled mechanisms, and it deserves further efforts to improve knowledge of this feedback in order to cope with the pandemic waves.

3.2. Model-predicted consequence of variable $\beta(t)$

The model-projected trajectories of variable $\beta(t)$, which represents the time-varying infection rate and reflects the behavioral response to the epidemic outbreak, are depicted in Figs. 3–5, along with the fitting curves of the actual data, in an attempt to compare its evolution with that of the infection waves.

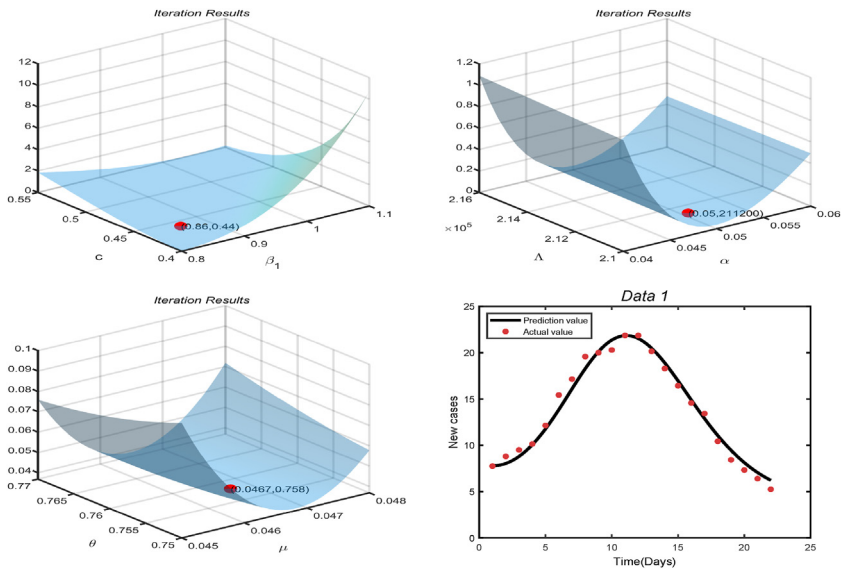

Fig. 2. Parameter estimation and simulated profile for Data 1.

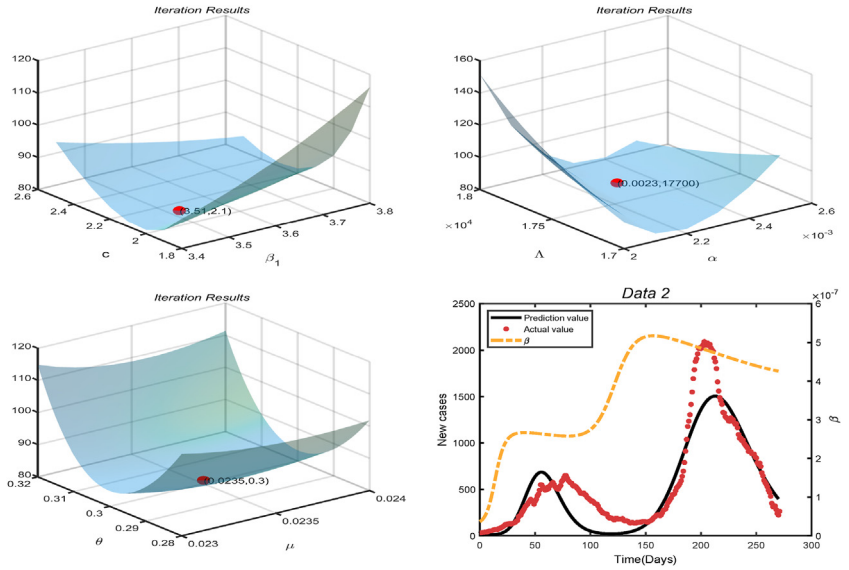

Fig. 3. Parameter estimation and simulated profile for Data 2.

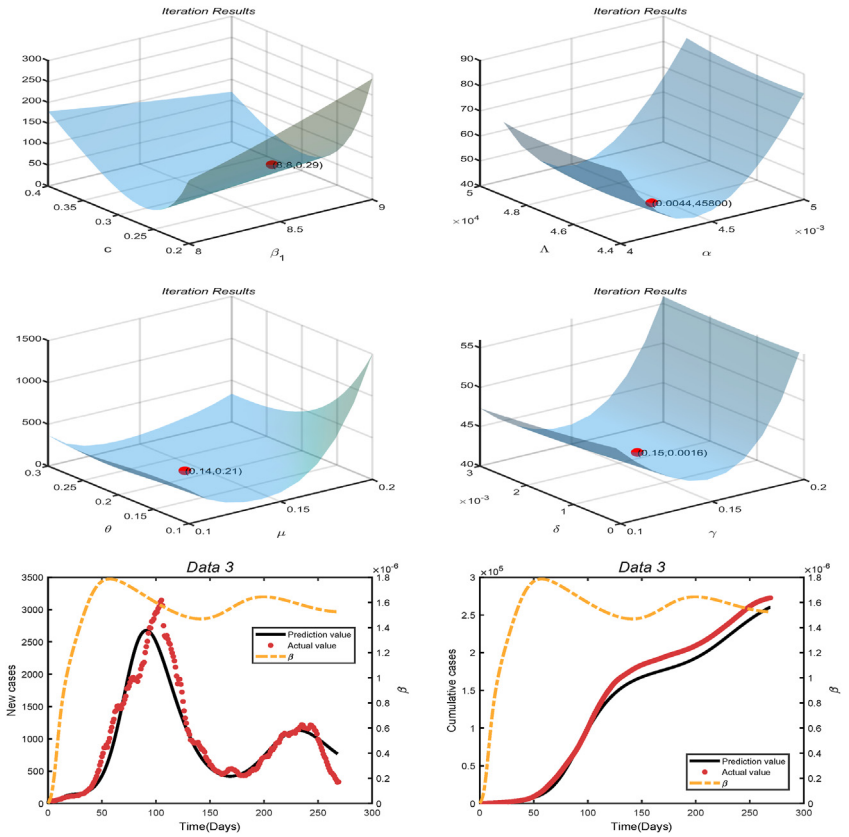

Fig. 4. Parameter estimation and simulated profile for Data 3.

As observed in the figures, the number of infected cases and $\beta(t)$ follow the same trends in their variations and exhibit a high correlation, which is consistent with the relationship between them. In particular, the fluctuations in the number of new cases give rise to a corresponding change in human behavior, in response to the changing prevalence of the disease.

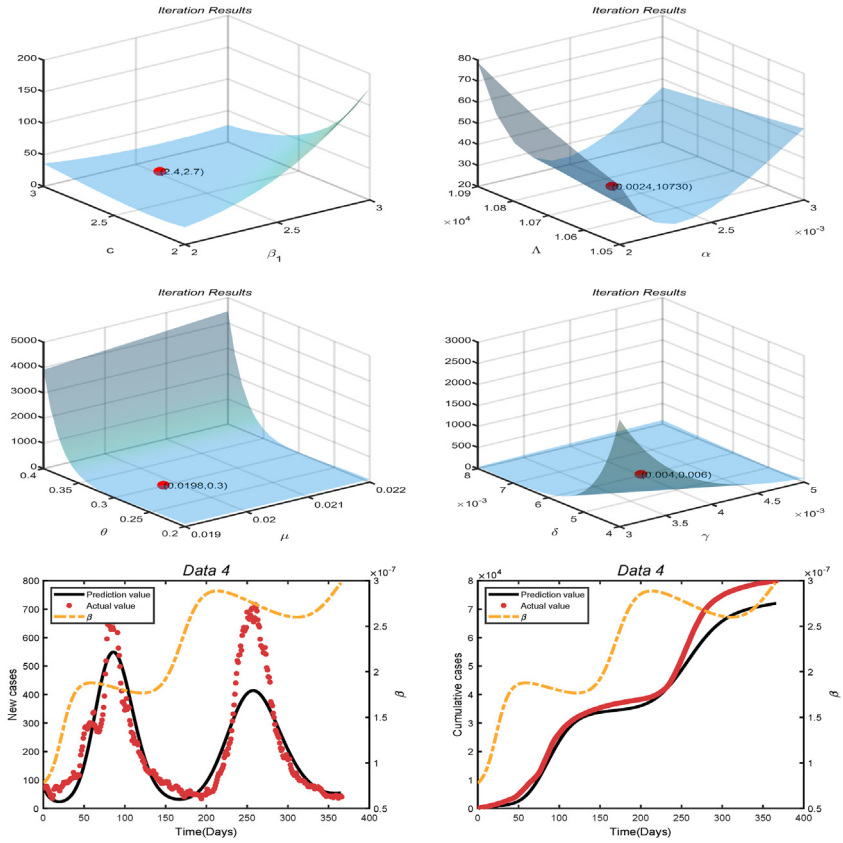

Fig. 5. Parameter estimation and simulated profile for Data 4.

Consequently, it can be observed that the value of $\beta(t)$ is subject to a state of continuous change. On the other hand, the variation of $\beta(t)$ will necessarily produce a feedback effect on the spread of the epidemic course, resulting in the severity or mitigation of the disease prevalence. In addition, it can be seen that there is a certain delay between the fluctuations of the variable $\beta(t)$ and the observed data, which seems reasonable since, for example, some time elapses before the new infected cases can be confirmed and reported.

3.3. *Effect of parameters related to behavioral response*

In order to examine the effect of behavior change on the disease transmission, the variations in infected population, triggered by the change of the two parameters α and c, which are closely related to the varying of variable $\beta(t)$ and the behavioral response, are simulated in Fig. 6 with the same parameters and values as in Fig. 3–5 for Data 2-Data 4. For a complete comparison and understanding, different scales of α and c are used to represent the profile of the model-simulated infections, as shown in Fig. 6.

Specifically, the comparison results related to Data 2 are depicted in the first row of Fig. 6, where the model-projected trajectories provide the predicted cases in terms of 0.6α, 0.8α, α and 1.2α, as well as that of c, in which α and c denote the corresponding values in the fitting curves in Fig. 3. From the trajectories we can see that, if α is decreased to 0.6α, implying that people are more reluctant to change their social behavior and also that it takes a longer time scale to reduce their social contacts, the simulated infections will experience a significant increase in the peak, from approximately 1500 cases to more than 3000 cases. Additionally, there is a slight delay in the peak time. Meanwhile, for the parameter c, it shows the similar performance in the evolution of the new cases, i.e., the lower it is, the higher the peak of the infections, observing that c is the inverse of the half-saturation constant, which reflects individuals' perceptions of the severity level of the epidemic and measures the impact of infected cases on behavior change. As expected, the model-projected outcomes for the newly infected population with varying α and c in Data 3 and Data 4 yield similar comparison results as in Data 2. However, in the absence of pharmaceutical interventions, the simulation results of the increased α and c in Data 4 also show that recurrent waves of the epidemic are still likely to occur even if the NPIs, such as the self-regulated and policy-driven behavior modifications, are implemented and the number of the new cases is reduced accordingly.

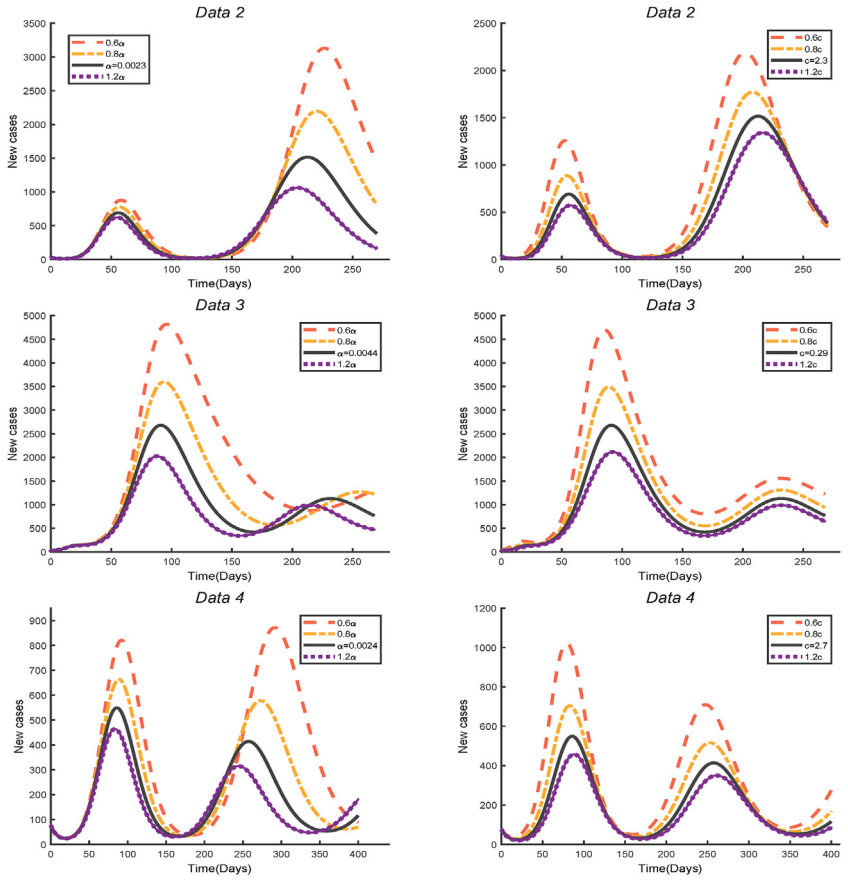

Fig. 6. The effect of α and c on the model-simulated infections.

4. Conclusion

Behavioral changes both at the institutional and personal level play an important role in affecting the epidemic course, such as leading to oscillations in the prevalence with varying numbers of peaks and lags during the epidemic outbreaks (shown in Fig. 6). Meanwhile, the hazard of infection potentially drives people to adopt protective behaviors in response to fluctuations in the contagion data, alternatively implementing or relaxing behavioral modifications at different risks of disease prevalence. Understanding the feedback effect between the dynamics of the epidemic progression and the behavioral response is important for control efforts, as presented in guiding public health interventions for COVID-19 pandemic, and it is therefore imperative to explore the underlying mechanisms of the coupled dynamics of behavioral response and epidemic outbreak, in order to assist in controlling and preventing the spread of infectious diseases. In modelling the features observed in the prevalence data of real pandemic, such as plateaus, shoulders, and oscillations, several recent works have discussed the effects of including behavior adaptation in the disease transmission dynamics (Brankston et al., 2024; Panicker & Sasidevan, 2024; Weitz, Park, Eksin, & Dushoff, 2023; Zhang et al., 2023).

In this study, we propose a SIR-β model by extending the classical SIR model, which would theoretically yield a single peak corresponding to when herd immunity is reached. And the independent variable $\beta(t)$, i.e., the time-varying rate of effective contact between individuals, has been introduced to characterise the feedback effect. Instead of incorporating other possible factors that influence the disease progression in model formulation, such as spatial effects, stochasticity, heterogeneity, and so on, we focus only on the nature of $\beta(t)$ due to its ability of fully accounting for public health responses in controlling epidemic outbreaks, which makes model (1) simple enough and capable of capturing the trend of selected COVID-19 data.

Our results show that such a feedback can have a significant effect on the trajectory of the epidemic dynamics. In fact, in order to obtain knowledge of the model parameters, we employ the PSO algorithm, which has its roots in the simulation of the collective behaviors of agents in swarms, to invert the parameter values in the solution procedures. The effectiveness of our proposed model was demonstrated by the fitting curves for the selected time series of COVID-19 data (shown in Figs. 2–5), where significant oscillations of different magnitude in the evolved trend were observed over the chosen time period. Although there exists obvious error and the match is not good enough, the simulated curves show similar patterns to

the real data. For parameters related to the behavioral response, we also examined how different levels of the response affect the waves of infection and the evolution of the disease.

Despite our exploration in modelling and the attempt to uncover the underlying mechanisms, it is admitted that the interaction between human behavior and disease transmission is complicated, as mentioned above. In response to the increasing spread of an epidemic, societies and individuals in different regions and countries act in different ways to contain its growth, and it is generally difficult to reproduce the exact course and provide the best solutions to real-world epidemiological problems. Therefore, it deserves more efforts to characterise the behavioral changes in transmission dynamic models. For example, except for the number of cases, the feedback effect may be directly driven by other stimulus, such as deaths, hospitalizations, or a combination of these, which may also be linked to "social memory" or "pandemic fatigue" (Bulai et al., 2023; Montefusco et al., 2023; Weitz et al., 2023). However, how to characterise the feedback effect in a simple model still remains a challenge, involving a delicate balance between incorporating complex social and behavioral phenomena and maintaining important modelling properties.

CRediT authorship contribution statement

Xinyu Chen: Writing – original draft, Visualization, Methodology, Formal analysis. **Suxia Zhang:** Writing – review & editing, Supervision, Methodology, Conceptualization. **Jinhu Xu:** Methodology, Conceptualization.

Data availability

All the data used to support the findings of this study are included in our manuscript and can be accessed freely from the references.

Declaration of competing interest

The authors declare that they have no known competing financial interests or personal relationships that could have appeared to influence the work reported in this paper.

Acknowledgments

This research was supported by National Natural Science Foundation of China (#62376212) and Scientific Research Program Project of Education Department of Shaanxi Province (#23JP114).

Appendix

For system (2), it always has a disease-free equilibrium $E_0 = (\frac{\Lambda}{\mu+\delta}, 0, \beta_0)$. The endemic level of the disease can be identified by finding the endemic equilibrium, denoted by $E^* = (S^*, I^*, \beta^*)$, where S^*, I^* and β^* are all positive and can be obtained by solving the following equations

$$\begin{aligned}
&\Lambda - \beta^* S^* I^* - (\mu+\delta)S^* = 0,\\
&\beta^* S^* I^* - (\mu+\theta+\gamma)I^* = 0,\\
&\frac{\beta_1}{1+cI^*} - \alpha\beta^* = 0.
\end{aligned}$$

Then we obtain

$$S^* = \frac{(\mu+\theta+\gamma)}{\beta^*},$$

$$I^* = \frac{\Lambda\beta^* - (\mu+\theta+\gamma)(\mu+\delta)}{(\mu+\theta+\gamma)\beta^*},$$

$$\beta^* = \frac{(\beta_1 + \alpha c(\mu+\delta))(\mu+\theta+\gamma)}{\alpha(\mu+\theta+\gamma+c\Lambda)},$$

noting that $I^* > 0$ if the basic reproduction number $\mathcal{R}_0 > 1$. In fact, substituting β^* into the expression of I^* leads to

$$I^* = \frac{\alpha(\mu+\theta+\gamma)(\mu+\delta)}{\beta_1(\mu+\theta+\gamma)+\Lambda c\alpha(\mu+\theta+\gamma)(\mu+\delta)}(\mathcal{R}_0-1).$$

Consequently, if $\mathcal{R}_0 > 1$, system (2) has a unique endemic equilibrium $E^* = (S^*, I^*, \beta^*)$.

Theorem 1. *If $\mathcal{R}_0 < 1$, the disease free equilibrium E_0 is locally asymptotically stable. Otherwise, it is unstable if $\mathcal{R}_0 > 1$.*

Proof. The Jacobian matrix of system (2) at E_0 is

$$J_0 = \begin{bmatrix} -b_2 & -\frac{\beta_1\Lambda}{\alpha b_2} & 0 \\ 0 & \frac{\beta_1\Lambda}{\alpha b_2} - b_1 & 0 \\ 0 & -c\beta_1 & -\alpha \end{bmatrix},$$

with $\mu+\theta+\gamma = b_1$ and $\mu+\delta = b_2$. Then the characteristic equation is as follows

$$(\lambda+b_2)(\lambda+\alpha)\left(\lambda+b_1-\frac{\beta_1\Lambda}{\alpha b_2}\right)=0.$$

Obviously, J_0 has two negative eigenvalues of $-b_2$ and $-\alpha$, and the remaining eigenvalue $\frac{\beta_1\Lambda}{\alpha b_2} - b_1$ is also negative if $\mathcal{R}_0 < 1$. By Routh-Hurwitz criterion, the disease-free equilibrium E_0 is locally asymptotically stable. Otherwise, if $\mathcal{R}_0 > 1$, E_0 is unstable due to the fact that $\frac{\beta_1\Lambda}{\alpha b_2} - b_1 > 0$.

In what follows, we examine the local stability of the endemic equilibrium E^* and we have the following theorem.

Theorem 2. *If $\mathcal{R}_0 > 1$, the unique endemic equilibrium E^* is locally asymptotically stable.*

Proof. The Jacobian matrix of system (2) at E^* is given by

$$J_1 = \begin{bmatrix} -\beta^* I^* - b_2 & -\beta^* S^* & -S^* I^* \\ \beta^* I^* & \beta^* S^* - b_1 & S^* I^* \\ 0 & -\frac{c\beta_1}{(1+cI^*)^2} & -\alpha \end{bmatrix},$$

Then the characteristic equation is as follows

$$\lambda^3 + H_2\lambda^2 + H_1\lambda + H_0 = 0, \tag{4}$$

where

$$H_2 = \beta^* I^* + b_2 + \alpha,$$
$$H_1 = \alpha(\beta^* I^* + b_2) + S^* I^* \frac{c\beta_1}{(1+cI^*)^2} + (\beta^*)^2 S^* I^*,$$
$$H_0 = b_2 S^* I^* \frac{c\beta_1}{(1+cI^*)^2}.$$

Clearly, $H_i > 0 (i = 1, 2, 3)$, and it is easy to check that $H_1H_2 - H_0 > 0$. Then Routh-Hurwitz criterion guarantees that every root of (4) has negative real part. Therefore, the endemic equilibrium E^* is locally asymptotically stable.

Theorem 3. *If $\mathcal{R}_0 < 1$, the disease-free equilibrium E_0 is globally asymptotically stable.*

Proof. Construct a Lyapunov function as

$$V_0(t) = S - S_0 - S_0 \ln\left(\frac{S}{S_0}\right) + I,$$

then we will show that $\frac{dV_0}{dt} \le 0$. Actually, calculating the derivative of V_0 along model (2) gives

$$\begin{aligned}\frac{dV_0}{dt} &= \left(1-\frac{S_0}{S}\right)\left(\Lambda-\beta SI-b_2S\right)+\beta SI-b_1I\\ &= \Lambda-\beta SI-b_2S-\frac{S_0}{S}\Lambda+\beta S_0I+b_2S_0+\beta SI-b_1I\\ &= b_2S_0\left(2-\frac{S_0}{S}-\frac{S}{S_0}\right)+\left(\beta\frac{\Lambda}{b_2}-b_1\right)I\\ &\le b_2S_0\left(2-\frac{S_0}{S}-\frac{S}{S_0}\right)+b_1(\mathcal{R}_0-1)I,\end{aligned}$$

thus $\frac{dV_0}{dt}\le 0$ is valid when $\mathcal{R}_0<1$. In addition, $\frac{dV_0}{dt}=0$ holds if and only if $S=S_0$ and $I=0$, which implies that the largest compact invariant set where $\frac{dV_0}{dt}=0$ is the singleton $\{E_0\}$. Therefore, by LaSalle invariance principle, the disease-free equilibrium E_0 is globally asymptotically stable. This completes the proof.

In order to examine the global stability of the endemic equilibrium E^*, let

$$A=\frac{\beta_1 c}{(1+cI)(1+cI^*)},$$

then it follows that

$$\frac{\beta_1 c}{(1+c\frac{\Lambda}{\mu})(1+cI^*)}\le A\le\frac{\beta_1 c}{1+cI^*}.$$

For convenience, denote

$$K_1=\frac{\beta_1 c}{(1+c\frac{\Lambda}{\mu})(1+cI^*)},\quad K_2=\frac{\beta_1 c}{1+cI^*}.$$

Assuming $a_i(i=1,2)\in\mathbb{R}^+$ and satisfying the following conditions

$$\begin{aligned}&\max\left\{\frac{\Lambda}{2\beta^*\mu},\frac{b_1^2}{b_2K_1}\right\}<a_1<\min\left\{\frac{\alpha\mu}{\beta^*\Lambda},\frac{2b_1\Lambda}{\beta^*\mu}\right\},\\ &\frac{\Lambda^2}{\alpha\mu^2}<\frac{a_2}{a_1}<\frac{\sqrt{\alpha K_1}-K_2-\alpha}{K_2}.\end{aligned}\tag{5}$$

Theorem 4. *If $\mathcal{R}_0>1$ and the inequalities (5) hold, then the endemic equilibrium E^* is globally asymptotically stable.*

Proof. Construct a Lyapunov function as

$$V_1(t)=\frac{1}{2}(S-S^*)^2+\frac{1}{2}a_1(I-I^*+\beta-\beta^*)^2+\frac{1}{2}a_2(\beta-\beta^*)^2.$$

Differentiating V_1 along system (2) yields

$$\begin{aligned}\frac{dV_1}{dt} &= -(S-S^*)(SI(\beta-\beta^*)+\beta^*I(S-S^*)+\beta^*S^*(I-I^*))-b_2(S-S^*)^2\\ &\quad -a_1(I-I^*+\beta-\beta^*)(\beta^*I(S^*-S)+SI(\beta^*-\beta))\\ &\quad -a_1(I-I^*+\beta-\beta^*)(\alpha(\beta-\beta^*)+A(I-I^*))\\ &\quad -a_2(\beta-\beta^*)(\alpha(\beta-\beta^*)+A(I-I^*))\\ &= a_1SI(\beta-\beta^*)^2-\beta^*I(S-S^*)^2-b_2(S-S^*)^2-\alpha a_1(\beta-\beta^*)^2-\alpha a_2(\beta-\beta^*)^2\\ &\quad -a_1A(I-I^*)^2-(\beta^*S^*-a_1\beta^*I)(S-S^*)(I-I^*)\\ &\quad -((a_1+a_2)A+a_1\alpha-a_1SI)(I-I^*)(\beta-\beta^*)\\ &\quad -(SI-a_1\beta^*I)(S-S^*)(\beta-\beta^*).\end{aligned}$$

After arranging the above expression, we obtain

$$\begin{aligned}\frac{dV_1}{dt} = &-\frac{1}{2}b_2\left(\left(S-S^*\right)+\frac{\beta^*S^*-a_1\beta^*I}{b_2}(I-I^*)\right)^2-\frac{1}{2}b_2\left(\left(S-S^*\right)+\frac{SI-a_1\beta^*I}{b_2}(\beta-\beta^*)\right)^2\\ &-\frac{1}{2}a_1A\left(\left(I-I^*\right)+\frac{(a_1+a_2)A+a_1\alpha-a_1SI}{a_1A}(\beta-\beta^*)\right)^2-\beta^*I(S-S^*)^2\\ &+\frac{1}{2}\frac{(\beta^*S^*-a_1\beta^*I)^2}{b_2}(I-I^*)^2-\frac{1}{2}a_1A(I-I^*)^2\\ &+\frac{1}{2}\frac{(SI-a_1\beta^*I)^2}{b_2}(\beta-\beta^*)^2-\frac{1}{2}\alpha a_1(\beta-\beta^*)^2\\ &+\frac{1}{2}\frac{((a_1+a_2)A+a_1\alpha-a_1SI)^2}{a_1A}(\beta-\beta^*)^2-\frac{1}{2}\alpha a_1(\beta-\beta^*)^2\\ &+a_1SI(\beta-\beta^*)^2-\alpha a_2(\beta-\beta^*)^2,\end{aligned}$$

Clearly, if the terms of the last four lines of the above $\frac{dV_1}{dt}$ are negative, especially if

$$\begin{aligned}&\frac{(\beta^*S^*-a_1\beta^*I)^2}{b_2}<a_1A,\\ &\frac{(SI-a_1\beta^*I)^2}{b_2}<\alpha a_1,\\ &\frac{((a_1+a_2)A+a_1\alpha-a_1SI)^2}{a_1A}<\alpha a_1,\\ &a_1SI<\alpha a_2,\end{aligned}$$

which can be guaranteed by

$$\frac{b_1^2}{b_2K_1}<a_1<\frac{2b_1\mu}{\beta^*\Lambda}, \tag{6}$$

$$\frac{\Lambda}{2\beta^*\mu}<a_1<\frac{\alpha\mu}{\beta^*\Lambda}, \tag{7}$$

$$a_2K_2<a_1(\sqrt{\alpha K_1}-K_2-\alpha), \tag{8}$$

$$a_1\frac{\Lambda^2}{\mu^2}<\alpha a_2, \tag{9}$$

respectively, then $\frac{dV_1}{dt}$ will be negative definite in the maximum positive invariant set Ω. Accordingly, the inequalities in (5) can be deduced by combining conditions (6)–(9). As a result, if the coefficients a_1 and a_2 in Lyapunov function V_1 can be taken appropriately to satisfy the inequalities in (5), then $\frac{dV_1}{dt}<0$ is satisfied, which leads to the fact that E^* is asymptotically global stability of. The proof is complete.

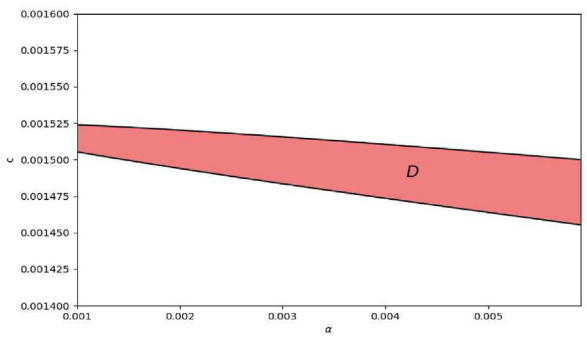

Fig. 7. Feasible region D constrained by condition (5).

Remark3. Fixing the parameters in model (2) except for α and c, the feasible set D is plotted numerically in Fig. 7 to verify that the parameter set satisfying the inequalities in (5) is not empty.

References

Agaba, G., Kyrychko, Y., & Blyuss, K. (2017). Mathematical model for the impact of awareness on the dynamics of infetious diseases. *Mathematical Biosciences, 286*, 22–30.

Azizi, A., Kazanci, C., Komarova, N. L., & Wodarz, D. (2022). Effect of human behavior on the evolution of viral strains during an epidemic. *Bulletin of Mathematical Biology, 84*, 144.

Bedson, J., Skrip, L. A., Pedi, D., Abramowitz, S., et al. (2021). A review and agenda for integrated disease models including social and behavioural factors. *Nature Human Behaviour, 5*, 834–846.

Brankston, G., Fisman, D. N., Poljak, Z., Tuite, A. R., et al. (2024). Examining the effects of voluntary avoidance behaviour and policy-mediated behaviour change on the dynamics of SARS-CoV-2: A mathematical model. *Infect. Dis. Model, 9*, 701–712.

Bulai, I. M., Montefusco, F., & Pedersen, M. G. (2023). Stability analysis of a model of epidemic dynamics with nonlinear feedback producing recurrent infection waves. *Applied Mathematics Letters, 136*, Article 108455.

Buonomo, B., Della Marca, R., & Sharbayta, S. S. (2022). A behavioral change model to assess vaccination-induced relaxation of social distancing during an epidemic. *Journal of Biological Systems, 30*, 1–25.

Cabrera, M., Córdova-lepe, F., Gutiéerrez-Jara, J. P., & Vogt-Geisse, K. (2021). An SIR-type epidemiological model that integrates social distancing as a dynamic law based on point prevalence and socio-behavioral factors. *Scientific Reports, 11*, Article 10170.

Capasso, V., & Serio, G. (1978). A generalization of the Kermack-Mckendrick deterministic eqidemic model. *Mathematical Biosciences, 42*, 43–61.

Cui, J., Sun, Y., & Zhu, H. (2008). The impact of media on the control of infectious diseases. *Journal of Dynamics and Differential Equations, 20*, 31–53.

Diagne, M. L., Agusto, F. B., Rwezaura, H., Tchuenche, J. M., et al. (2024). Optimal control of an epidemic model with treatment in the presence of media coverage. *Scientific African, 24*, Article e02138.

Fome, A. D., Rwezaura, H., Diagne, M. L., Collinson, S., et al. (2023). A deterministic Susceptible-Infected-Recovered model for studying the impact of media on epidemic dynamics. *Healthc. Anal., 3*, Article 100189.

Funk, S., Gilad, E., & Jansen, V. A. A. (2010). Endemic disease, awareness, and local behavioural response. *Journal of Theoretical Biology, 264*, 501–509.

Gilbert, M., Pullano, G., Pinotti, F., Valdano, E., et al. (2020). Preparedness and vulnerability of african countries against importations of COVID-19: A modelling study. *Lancet, 395*, 871–877.

Haug, N., Geyrhofer, L., Londei, A., Dervic, E., et al. (2020). Ranking the effectiveness of worldwide COVID-19 government interventions. *Nature Human Behaviour, 4*, 1303–1312.

Hethcote, H. W. (2000). The mathematics of infectious diseases. *SIAM Review, 42*, 599–653.

Jain, K., Bhaunagar, V., Prasad, S., & Kaur, S. (2023). Coupling fear and contagion for modeling epidemic dynamics. *IEEE Trans. Netw. Sci. Eng., 10*, 20–34.

Kermack, W. O., & McKendrick, A. G. (1927). A contribution to the mathematical theory of epidemics. *Proceedings of the Royal Society of London, 115*, 700–721.

Kolokolnikov, T., & Iron, D. (2021). Law of mass action and saturation in SIR model with application to coronavirus modelling. *Infect. Dis. Model, 6*, 91–97.

Laarabi, H., Rachik, M., Kahlaoui, O. E., & Labriji, E. H. (2013). Optimal vaccination strategies of an SIR epidemic model with a saturated treatment. *Univ. J. Appl. Math., 1*, 185–191.

Liu, R., Wu, J., & Zhu, H. (2007). Media/psychological impact on multiple outbreaks of emerging infectious diseases. *Computational and Mathematical Methods in Medicine, 8*, 153–164.

Montefusco, F., Procopio, A., Bulai, I. M., Amato, F., et al. (2023). Interacting with COVID-19: How population behavior, feedback and memory shaped recurrent waves of the epidemic. *IEEE Control Syst. Lett., 7*, 583–588.

Panicker, A., & Sasidevan, V. (2024). Social adaptive behavior and oscillatory prevalence in an epidemic model on evolving random geometric graphs. *Chaos, Solitons & Fractals, 178*, Article 114407.

Rubin, G. J., Amlôt, R., Page, L., & Wessely, S. (2009). Public perceptions, anxiety, and behaviour change in relation to the swine flu outbreak: Cross sectional telephone survey. *BMJ, 339*, Article b2651.

Sardar, T., Nadim, S. S., & Rana, S. (2023). Detection of multiple waves for COVID-19 and its optimal control through media awareness and vaccination: Study based on some Indian states. *Nonlinear Dynamics, 111*, 1903–1920.

Song, P., & Xiao, Y. (2019). Analysis of an epidemic system with two response delays in media impact function. *Bulletin of Mathematical Biology, 81*, 1582–1612.

Song, P., & Xiao, Y. (2022a). Estimating time-varying reproduction number by deep learning techniques. *J. Appl. Anal. Comput., 12*, 1077–1089.

Song, P., & Xiao, Y. (2022b). Analysis of a diffusive epidemic system with spatial heterogeneity and lag effect of media impact. *Journal of Mathematical Biology, 85*, 17.

Stolerman, L. M., Coombs, D., & Boatto, S. (2015). SIR-network model and its application to dengue fever. *SIAM Journal on Applied Mathematics, 75*, 2581–2609.

Sun, C., Yang, W., Arino, J., & Khan, K. (2011). Effect of media-induced social distancing on disease transmission in a two patch setting. *Mathematical Biosciences, 230*, 87–95.

Tang, B., Zhou, W., Wang, X., Wu, H., & Xiao, Y. (2022). Controlling multiple COVID-19 epidemic waves: An Insight from a multi-scale model linking the behaviour change dynamics to the disease transmission dynamics. *Bulletin of Mathematical Biology, 84*, 106.

Tchuenche, J. M., & Bauch, C. T. (2012). Dynamics of an infectious disease where media coverage influences transmission. *ISRN Biomath, 2012*, Article 581274.

Tchuenche, J. M., Dube, N., Bhunu, C. P., Smith, R. J., et al. (2011). The impact of media coverage on the transmission dynamics of human influenza. *BMC Public Health, 11*(S1), S5.

Teslya, A., Pham, T. M., Godijk, N. G., Kretzschmar, M. E., et al. (2020). Impact of self-imposed prevention measures and short-term government-imposed social distancing on mitigating and delaying a covid-19 epidemic: A modelling study. *PLoS Medicine, 17*, Article e1003166.

Vrugt, M. T., Bickmann, J., & Wittkowski, R. (2021). Containing a pandemic: Nonpharmaceutical interventions and the "second wave". *J. Phys. Commun., 5*, Article 55008.

Wang, X., Wu, H., & Tang, S. (2022). Assessing age-specific vaccination strategies and post-vaccination reopening policies for COVID-19 control using SEIR modeling approach. *Bulletin of Mathematical Biology, 84*, 108.

Wang, X., & Zhang, S. (2024). Coupling media coverage and susceptibility for modeling epidemic dynamics: An application to COVID-19. *Mathematics and Computers in Simulation, 217*, 374–394.

Weitz, J. S., Park, S. W., Eksin, C., & Dushoff, J. (2023). Avareness-driven behavior changes can shift the shape of epidemics away from peaks and toward plateaus, shoulders, and oscillations. *Proceedings of the National Academy of Sciences, 117*, 32764–32771.

World Health Organization. https://covid19.who.int/.

Xiao, Y., Tang, S., & Wu, J. (2015). Media impact switching surface during an infectious disease outbreak. *Scientific Reports, 5*, 7838.

Yerlanov, M., Agarwal, P., Colijn, C., & Stockdale, J. E. (2023). Effective population size in simple infectious disease models. *Journal of Mathematical Biology, 87*, 80.

Yin, S., Wu, J., & Song, P. (2023). Optimal control by deep learning techniques and its applications on epidemic models. *Journal of Mathematical Biology, 86*, 36.
Zhang, X., Scarabel, F., Murty, K., & Wu, J. (2023). Renewal equations for delayed population behaviour adaptation coupled with disease transmission dynamics: A mechanism for multiple waves of emerging infections. *Mathematical Biosciences, 365*, Article 109068.
Zhou, Y., Rahman, M. M., Khanam, R., & Taylor, B. R. (2023). Individual preferences, government policy, and COVID-19: A game-theoretic epidemiological analysis. *Applied Mathematical Modelling, 122*, 401–416.
Zuo, C., Ling, Y., Zhu, F., Ma, X., & Xiang, G. (2023). Exploring epidemic voluntary vaccinating behavior based on information-driven decisions and benefit-cost analysis. *Applied Mathematics and Computation, 447*, Article 127905.